Research Square

Preprints are preliminary reports that have not undergone peer review.
They should not be considered conclusive, used to inform clinical practice,
or referenced by the media as validated information.

Disparities in Microscale Pedestrian Environment Features by Income and Demographic Context Across Four U.S. Regions

Zahra Mohammadibalini

zmoham21@asu.edu

Arizona State University - Downtown Phoenix Campus https://orcid.org/0009-0001-5800-0738

Akshar Patel

Arizona State University - Downtown Phoenix Campus

Christine B. Phillips

Clemson University

Lawrence D. Frank

University of California San Diego

Marc A. Adams

Arizona State University - Downtown Phoenix Campus

Research Article

Keywords: built environment, walkability, microscale pedestrian environment feature, health equity, computer vision, street view imagery

Posted Date: November 25th, 2026

DOI: https://doi.org/10.21203/rs.3.rs-11779023/v1

License: This work is licensed under a Creative Commons Attribution 4.0 International License.
Read Full License

Disparities in Microscale Pedestrian Environment Features by Income and Demographic Context Across Four U.S. Regions

Zahra Mohammadibalini[a,*], Akshar Patel[a], Christine B. Phillips[b,c], Lawrence D. Frank[d], Marc A. Adams[a]

[a] College of Health Solutions, Arizona State University, 425 N. 5th Street, Phoenix, AZ 85004, USA

[b] Department of Psychology, Clemson University, 418 Brackett Hall, Clemson, SC 29634, USA

[c] Institute for Engaged Aging, Clemson University, 298 Memorial Drive, Seneca, SC 29672, USA

[d] Department of Urban Studies and Planning, University of California San Diego, 9500 Gilman Drive, La Jolla, CA 92093, USA

[*] **Corresponding author:** Zahra Mohammadibalini, College of Health Solutions, Arizona State University, 425 N. 5th Street, Phoenix, AZ 85004, USA. Email: zmoham21@asu.edu

Abstract:

Walking-supportive neighborhoods are important for population health, yet macroscale walkability indices can obscure street-level conditions and their equitable distribution. This cross-sectional study explored how neighborhood income and demographic composition relate to microscale pedestrian infrastructure and whether these income-related differences in microscale features are moderated by macroscale walkability. Nine microscale pedestrian environment features (PEFs) were measured from omnidirectional imagery using previously validated computer vision classifiers. We evaluated the percentage of PEF coverage for 5,509 census block groups (20,617,864 images, 5,154,466 coordinates) across four U.S. regions. Multivariable linear models regressed each feature on median household income, the National Walkability Index, their interaction, and demographic and regional covariates. Walkability was positively associated with every feature (all $p < .001$). The income × walkability interaction was significant for eight of nine features ($p < .05$): in the most walkable neighborhoods, higher income predicted greater coverage of basic walking infrastructure (sidewalks, curb cuts, buffers; e.g., sidewalks $B = 0.081$, $p < .001$), but lower coverage of marked crossings, walk signals, and benches (e.g., walk signals $B = -0.045$, $p < .001$); streetlights showed a uniform negative gradient with income. Patterns were largely robust to outlier-handling and bootstrap analyses. Neighborhoods that appear most walkable, therefore, do not uniformly provide the most equitable street-level environments; pedestrian infrastructure equity should be assessed feature by feature, helping planners and transportation agencies target investment where pedestrian need is greatest rather than assuming adequacy where macroscale walkability is high, particularly given elevated pedestrian fatality risk in lower-income areas.

Keywords: built environment; walkability; microscale pedestrian environment feature; health equity; computer vision; street view imagery

1. Introduction

Neighborhood environments that support walking are important determinants of urban health. Built environment characteristics such as walkability, street connectivity, active transportation infrastructure, and parks are generally associated with physical activity and active travel, although evidence varies by study design, population, and outcome [1-4]. Most walkability research relies on macroscale indicators such as density, land-use mix, street connectivity, and destination and transit access, often summarized in indices such as Walk Score and the National Walkability Index [3, 5-7]. These measures capture whether neighborhoods are structurally supportive of walking, but not the street-level features pedestrians directly experience, such as sidewalks or crosswalks [1, 8, 9]. Microscale pedestrian environment features (PEFs) are less costly and more readily modifiable than macroscale features through local planning, transportation, and public works decisions, and studies using the Microscale Audit of Pedestrian Streetscapes show that they are associated with walking, biking, and physical activity across age groups, even after accounting for macroscale walkability [10-12].

Access to PEFs is a social determinant of health because pedestrian infrastructure shapes who has safe, convenient opportunities to walk. Evidence on how these features vary by neighborhood income and racial/ethnic composition is mixed. Several studies report that low-income or racially/ethnically minoritized neighborhoods have poorer aesthetics, more physical disorder, worse sidewalk conditions, fewer safety-supportive features, or lower perceived neighborhood quality [1, 13-15], whereas others find better accessibility, more destinations, or selected pedestrian amenities in such neighborhoods, depending on the feature and local context [1, 6, 16]. For example, Thornton et al. [16] found poorer aesthetic and social features in lower-income and higher-minority neighborhoods, but worse or absent sidewalks, crosswalks, and intersections in some higher-income and lower-minority neighborhoods. PEF inequities should therefore be examined feature by feature rather than assumed to follow a single income or racial/ethnic gradient [16, 17]. A recent national study showed that lower-income, disadvantaged communities systematically experience higher macroscale walkability along with poorer environmental exposures, including increased air pollution, reduced tree canopy, and increased injury

risk, perhaps due to a lack of pedestrian infrastructure [8]. Lower-income communities are more transit- and pedestrian-dependent, suggesting likely highly disproportionate exposure to injury risk [18].

A key challenge is that macroscale walkability may mask microscale inequities: disadvantaged neighborhoods may appear walkable on density, connectivity, or access-based measures while having poorer street-level safety, comfort, maintenance, and perceived quality [1, 6, 8, 9]. In Los Angeles, disadvantaged neighborhoods appeared more walkable at the macro level, but street greenery, sidewalk quality, and perceived safety revealed less supportive walking environments [9]; similarly, higher-poverty and non-White neighborhoods had better access to destinations and recreational space but were less safe and comfortable for outdoor physical activity [1]. Examining microscale PEFs while accounting for macroscale walkability is therefore necessary to determine whether walkable-appearing neighborhoods also provide equitable street-level infrastructure.

Measuring microscale PEFs across large areas has been difficult: in-person streetscape audits are time-consuming, costly, geographically limited, and expose raters to traffic risks, and virtual audits of omnidirectional imagery, such as Google Street View or Mapillary, reduce these burdens but still require substantial trained labor [19-22]. Computer vision applied to street-view imagery offers a scalable alternative [19-21]: models have been developed to detect multiple microscale walkability features, including sidewalks, sidewalk buffers, curb cuts, zebra and line crosswalks, walk signals, bike symbols, and streetlights [19], and large-scale applications have linked image-derived built environment indicators to public health and equity questions [21, 23-25]. In St. Louis, for example, a vision–language model applied to street-view imagery showed that higher-income census tracts had more continuous pavement and better-maintained buildings [26]. However, few studies have assessed multiple PEFs simultaneously across several U.S. regions using computer vision [16, 19, 20], even though disparities vary by feature type, measurement scale, and regional context [6, 9, 16]. Accordingly, this study examines how neighborhood income, racial/ethnic composition, and other demographic

characteristics are associated with nine computer vision–derived PEFs within and across four U.S. regions, and whether the income–coverage association is moderated by macroscale walkability.

2. Materials and Methods

2.1. Study Design and Setting

This cross-sectional study was conducted across four U.S. regions: Maricopa County (Phoenix region), San Diego County (San Diego region), King County (Seattle region), and Baltimore City and County (Baltimore region). The census block group was the unit of analysis, as it is small enough to capture neighborhood-level variation while still linking to sociodemographic and environmental data [27, 28]. The regions were chosen for two reasons: the classifiers had been developed on a smaller subset of omnidirectional imagery from these areas [19], so applying them at scale in the same regions supported detection validity, and the regions differ in geography, climate, urban form, and sociodemographic composition, from Baltimore's older urban fabric to Phoenix's newer, automobile-oriented development, allowing patterns to be examined across varied contexts rather than in a single city. Fig. 1 shows the study regions and the distribution of National Walkability Index scores across their block groups.

2.2. Outcomes: Microscale Pedestrian Environment Features (PEFs)

The study outcomes were the presence of nine microscale PEFs: sidewalks, sidewalk buffers, curb cuts, line crosswalks, zebra crosswalks, walk signals, bike symbols, streetlights, and benches. PEFs were detected using previously validated computer vision classifiers, originally trained on over 100,000 images with the EfficientNetB5 architecture and applied only to the home neighborhoods of 512 WalkIT Arizona participants in a single region [19]. For this study, the models were retrained on additional labeled omnidirectional images from the four regions and multiple image sources, selected across high- and low-walkability and high- and low-income block groups, which improved classification performance relative to the original models (Adams et al., manuscript in preparation). A bench classifier was also trained and validated, addressing a feature Adams et al. [19] had identified as a future direction, because benches allow people to rest.

Omnidirectional images from Google Street View and Mapillary were sampled at approximately 15-m intervals along street segments and at intersections, with four directional images (0°, 90°, 180°, and 270°) retrieved at each sampled point. After duplicate captures were removed from the 21,375,677 images initially retrieved, the sample comprised 5,154,466 unique sampling coordinates and 20,617,864 images (Supplementary Table S1). At each coordinate, the maximum predicted score for each PEF across the four directional images was retained, and a feature was classified as present when this maximum exceeded 50% probability. Each outcome was then calculated as the percentage of eligible sampled points in a block group at which the feature was present (eligibility is defined below).

Four PEFs—curb cuts, line crosswalks, zebra crosswalks, and walk signals—are intersection-specific and were therefore derived only from sampling points within 25 m of a street intersection, identified from 2024 TIGER/Line street data [29]; this radius exceeds the approximately 15-m sampling interval, helping to ensure at least one sampled point per intersection, and accommodates wider multilane arterials. Intersection points represented 29.0% of all sampled points. The other five PEFs were derived from all sampled points.

2.3. Predictor Variables

All predictors were measured at the census block group level; sociodemographic variables were obtained from the 2019–2023 American Community Survey (ACS) 5-Year Estimates [30]. The primary predictor was median household income, modeled continuously in $10,000 increments. Macroscale walkability was measured with the U.S. Environmental Protection Agency National Walkability Index, derived from Smart Location Database indicators of street intersection density, transit proximity, and land-use diversity, scored from 1 (least walkable) to 20 (most walkable), and entered as a continuous predictor [31, 32].

Additional covariates captured demographic dimensions linked to pedestrian infrastructure disparities in prior research: the Hispanic/Latino-to-non-Hispanic/Latino and non-White-to-White population ratios [1, 6, 16] and the percentage of residents aged 65 years and older [15, 19]. Sex ratio (males per 100 females, as reported in the ACS) was included as a demographic control, following prior built-environment equity analyses [24], and region was dummy-coded

with Phoenix as the reference. For graphical presentation only, walkability was also grouped into the agency's four categories: least, below-average, above-average, and most walkable [31].

2.4. Spatial Data Processing and Analytic Sample

Spatial data were processed in ArcGIS Pro version 3.4.0. ACS sociodemographic data and National Walkability Index values were joined to 2023 census block group cartographic boundary shapefiles [33]. Each sampling coordinate was spatially joined to the block group within which it fell. The analytic sample comprised 5,509 census block groups with analyzable omnidirectional imagery and complete ACS data and was used for all regression models.

2.5. Statistical Analysis

Statistical analyses were conducted in IBM SPSS Statistics version 29.0.1.0. Categorical variables were summarized as frequencies and percentages, and continuous variables as the mean (SD) when approximately symmetric (|skewness| < 0.5) [34] or otherwise as the median (Q1–Q3; Table 1; Supplementary Methods).

For each of the nine PEF outcomes, two multiple linear regression models were estimated: a main-effects model including income, walkability, and the covariates described in Section 2.3, and an interaction model that additionally included the income × walkability product term. Because neither income nor walkability has a meaningful zero, both were mean-centered before forming the product term; consequently, their lower-order coefficients represent associations at the sample mean of the other variable [35], and the nonessential multicollinearity between the interaction term and its components is reduced [36]. Unstandardized coefficients (B), 95% confidence intervals, p-values, R^2, adjusted R^2, and the ΔR^2 attributable to the interaction term were reported, and multicollinearity was assessed using variance inflation factors. Interaction models are presented in the main text (Table 2) and main-effects models in Supplementary Table S2.

2.6. Sensitivity Analysis

To assess robustness, the nine interaction models were re-estimated in three alternative samples. The first, an extreme-ratio screen, excluded 326 block groups (5.9%) with implausible demographic ratios as likely error outliers [37]. The second, a Cook's-distance specification,

excluded 1,052 block groups (19.1%) identified as influential ($D > 4/n$) and was interpreted as a conservative, worst-case bound [37-39]. The third, a minimum-imagery screen, excluded 21 block groups (0.4%) with fewer than five sampled points [9]. Because the skewed, zero-bounded outcomes may violate the ordinary least squares assumptions, 95th-percentile confidence intervals for the interaction coefficients were also obtained from a nonparametric case-resampling bootstrap with 2,000 replicates [40]; an interaction was considered robust when this interval excluded zero. Thresholds and their rationale are given in the Supplementary Methods, and results in Supplementary Tables S3 and S4.

3. Results

3.1. Descriptive Characteristics

The analytic sample (N = 5,509; Table 1) was nearly half Phoenix (48.1%) and predominantly walkable (70.2% above-average or most walkable), with a median household income of $95,227 (Q1–Q3: $67,126–$132,323). The nine PEFs differed markedly in prevalence: sidewalks and streetlights were near-ubiquitous (medians 89.67% and 70.45%), whereas line crosswalks, walk signals, benches, bike symbols, and zebra crosswalks had medians below 5%, so percentage-point differences are proportionally larger for these features. Regional patterns diverged: Seattle had the highest average walkability (15.57) but the lowest sidewalk (81.26%) and curb-cut (41.34%) coverage, whereas Phoenix had the lowest walkability (11.13) but the highest sidewalk (93.65%) and streetlight (78.60%) coverage. Crosswalk marking style also varied by region: zebra crosswalks were effectively absent in Phoenix but dominant in Seattle, where line crosswalks were absent.

3.2. Adjusted Associations of Walkability and Income with Feature Coverage

In the interaction models (Table 2), coefficients are expressed in percentage points. Walkability was positively associated with coverage of every feature at mean income (e.g., sidewalks B = 1.76 per index point, 95% CI 1.58 to 1.94; streetlights B = 1.27, 95% CI 1.11 to 1.42; all $p < .001$). At mean walkability, higher income was associated with lower coverage of streetlights (B = −0.75 per $10,000, 95% CI −0.86 to −0.65), walk signals (B = −0.32, 95% CI −0.38 to −0.25), line crosswalks (B = −0.21), zebra crosswalks (B = −0.12), and benches (B = −0.04)

(all $p < .001$), but with greater buffer coverage ($B = 0.38$, 95% CI 0.24 to 0.52, $p < .001$); income was not significantly associated with sidewalk, curb-cut, or bike-symbol coverage at mean walkability. Model fit ranged from $R^2 = 0.09$ (bike symbols) to $R^2 = 0.34$ (zebra crosswalks).

3.3. Income × Walkability Interactions

The income × walkability interaction was statistically significant for eight of the nine features (all except streetlights; Table 2). Although the interaction terms added only a small share of variance ($\Delta R^2 = 0.001–0.005$), they reversed the direction or amplified the magnitude of the income gradient across walkability categories (Fig. 2a–i). Three patterns emerged.

First, for sidewalks, buffers, and curb cuts (Fig. 2a, b, f), higher walkability was associated with a more positive income gradient (positive interactions). For sidewalks ($B = 0.081$, 95% CI 0.050 to 0.113, $p < .001$), higher income was associated with lower coverage in the least and below-average walkable categories but higher coverage in the most walkable category, reversing the gradient (Fig. 2a). Curb cuts showed the same, though smaller, reversal ($B = 0.033$, 95% CI 0.007 to 0.058, $p = .012$; Fig. 2f). For buffers ($B = 0.044$, 95% CI 0.009 to 0.079, $p = .014$), the positive interaction reflected amplification rather than reversal: buffer coverage increased with income in all four walkability categories and most steeply in the most walkable category (Fig. 2b).

Second, for streetlights, the interaction was not significant ($B = 0.022$, 95% CI −0.004 to 0.049, $p = .095$): predicted coverage declined with higher income at a similar rate across all walkability categories (Fig. 2d). *Third*, for bike symbols, benches, line crosswalks, zebra crosswalks, and walk signals (Fig. 2c, e, g–i), higher walkability was associated with a more negative income gradient (negative interactions). This pattern was most pronounced for walk signals ($B = −0.045$, 95% CI −0.061 to −0.029, $p < .001$), for which the decline in coverage with higher income was steepest in the most walkable category and comparatively flat in the least walkable category (Fig. 2i). Benches ($B = −0.006$), line crosswalks ($B = −0.033$), and zebra crosswalks ($B = −0.016$) (all $p < .01$) showed the same structure, with the income-related decline concentrated in the more walkable categories (Fig. 2e, g, h). Bike symbols showed a related reversal

(B = −0.006, 95% CI −0.010 to −0.001, p = .017): higher income was associated with greater coverage in the less-walkable categories but with flat to slightly lower coverage in the most-walkable category (Fig. 2c).

These interaction patterns were largely robust (Supplementary Tables S3 and S4). All eight significant interactions retained their direction in every sensitivity sample, and six remained significant in all three; the buffer interaction attenuated to non-significance under the extreme-ratio screen and the curb-cut interaction under both the extreme-ratio and Cook's-distance specifications. Bootstrap 95% confidence intervals excluded zero for six of the eight interactions but narrowly included zero for bike symbols (−0.012 to 0.001) and zebra crosswalks (−0.036 to 0.003).

3.4. Demographic and Regional Differences

Independent of income and walkability, several compositional characteristics were associated with feature coverage (Table 2; all reported associations $p < .05$). A higher percentage of residents aged 65 and older was associated with lower coverage of sidewalks (B = −0.06), buffers (B = −0.17), bike symbols (B = −0.006), streetlights (B = −0.18), and curb cuts (B = −0.11) but with greater line crosswalk coverage (B = 0.03). A higher Hispanic/Latino-to-non-Hispanic/Latino ratio was associated with lower buffer (B = −0.44), bike-symbol (B = −0.07), and walk-signal (B = −0.16) coverage, whereas a higher non-White-to-White ratio was associated with modestly greater sidewalk (B = 0.03), buffer (B = 0.03), and curb-cut (B = 0.02) coverage; the sex ratio showed only small associations ($|B| \leq 0.005$).

Regional differences were large and feature-specific (all reported $p < .001$). Relative to Phoenix, the other three regions had lower sidewalk and streetlight coverage (largest in Seattle: B = −16.14 and −17.00) but greater buffer coverage (largest in Baltimore: 36.49); Seattle also had lower curb-cut coverage (−16.72), and zebra crosswalks were more prevalent outside Phoenix, especially in Seattle (15.65).

4. Discussion

Three findings stand out. First, macroscale walkability was positively associated with coverage of all nine PEFs, indicating that it broadly tracks street-level pedestrian infrastructure. Second,

the association between income and feature coverage was feature-specific and, for eight of the nine features, conditional on walkability. Third, and most importantly, the direction of the income gradient within the most walkable neighborhoods diverged sharply across feature types. Neighborhoods appearing most pedestrian-supportive on a macroscale index therefore do not uniformly provide the most equitable street-level environments [8, 9].

For basic walking infrastructure—sidewalks, curb cuts, and sidewalk buffers—income gradients became more positive as walkability increased. One plausible interpretation is that, within highly walkable areas, surface infrastructure reflects the capital investment and maintenance regimes of affluent areas, which sustain continuous, well-maintained sidewalks, landscaped buffers, and accessible curb ramps in both newer developments built to current standards and older affluent neighborhoods whose pre-automobile sidewalks have been maintained and retrofitted. This is consistent with evidence that buffered sidewalks tend to concentrate in more affluent, lower-traffic-exposure environments [41] and that higher-income tracts have more continuous pavement [26]. Because curb cuts and buffers only occur where sidewalks exist, the parallel gradients should be read as a coherent pattern in surface infrastructure rather than three independent associations.

In contrast, for walking safety or amenity features—line and zebra crosswalks, walk signals, benches, and bike symbols—income gradients became more negative as walkability increased. A likely explanation is that this infrastructure is installed in response to pedestrian demand and traffic exposure rather than neighborhood affluence: walking in lower-income neighborhoods is more often utilitarian and concentrated along higher-volume arterials, whose hazards are substantially greater in these environments, whereas in higher-income neighborhoods it is more often recreational [41]. Transportation agencies may therefore prioritize marked crossings, walk signals, and transit-oriented amenities in denser, transit-served areas and near transit stops, where crossing needs and collision risk are highest—producing more of these features where macroscale walkability and lower income coincide. This pattern runs counter to the narrative that disadvantage means deficit.

Streetlights were the single exception to this walkability-conditional patterning: higher-income block groups showed uniformly lower streetlight coverage, with no significant variation by walkability. This is consistent with prior streetscape audits, in which adequate lighting was more prevalent in lower-income and higher-minority neighborhoods [16] and may reflect that street lighting tracks busier streets, density, and urban-core environments rather than the pedestrian-supportiveness captured by a walkability index.

These divergent patterns reinforce a growing recognition that macroscale walkability can mask microscale inequities and that "walkable" environments are not experienced equally across sociodemographic groups [1, 6, 8, 9]. Recent national evidence indicates that walkability–walking associations are weaker for Black, Hispanic, and lower-income residents [42] and that the same index can carry opposite implications across income groups, depending on whether the environment is assessed at the macro or micro scale [43, 44]. Our feature-level interaction results extend this literature by showing that, within a single macro-walkable context, income operates in opposite directions depending on whether the feature is a basic walking surface or a safety crossing/amenity element. Moreover, because the sidewalk and curb-cut income gradients reversed across walkability levels, they may cancel out when walkability is ignored, possibly explaining why a recent single-city analysis found no income association with pavement presence or curb ramps [26].

Demographic composition also did not follow a single disadvantage gradient: a higher non-White-to-White ratio was associated with modestly greater sidewalk, buffer, and curb-cut coverage, whereas a higher Hispanic/Latino-to-non-Hispanic/Latino ratio was associated with lower buffer, bike-symbol, and walk-signal coverage. These opposing directions caution against treating "minority" neighborhoods as a monolithic category, consistent with evidence that built-environment advantages and disadvantages vary by racial/ethnic group and feature [1, 16, 24] and that the mechanisms linking marginalization to walking differ by race versus income [42]. Regional patterns were likewise distinctive rather than uniformly stronger or weaker, echoing findings that the features driving disparities vary across metropolitan areas and that single-city studies are therefore limited in generalizability [16, 17].

Because microscale features are readily modifiable, these findings point to concrete, location- and feature-specific planning targets: investment should be matched to pedestrian need—volume, crossing risk, and accessibility—rather than assumed adequate wherever macroscale walkability is high. Considerable latent pedestrian demand for utilitarian travel may exist in lower-income, macroscale-walkable areas and may vary by feature. However, these implications also extend to more affluent areas that lack pedestrian infrastructure for both recreational and utilitarian travel. The basic features that were less common in lower-income, highly walkable block groups—sidewalks, curb cuts, and buffers—are essential for pedestrian safety. Residents of disadvantaged areas that lack basic, life-protective pedestrian features often walk out of necessity rather than choice [18], and lower-income areas experience higher rates of pedestrian injury and death [45]. Nationally, pedestrian fatality rates in census tracts with median household incomes of $15,000–$24,999 were more than four times those in tracts with incomes above $100,000 [46]. Among our study regions, pedestrian fatality rates in 2018–2022 were highest in the Phoenix (3.10 per 100,000 per year) and San Diego (2.83) metropolitan areas, both among the 30 deadliest U.S. metropolitan areas for people walking, followed by Baltimore (2.21) and Seattle (1.63), compared with a national rate of 2.06 [46].

Although the lower crossing and walk-signal coverage in higher-income, highly walkable block groups is consistent with provision tracking need, agencies should confirm that provision matches need across the full income range, since the same pattern could also reflect historical investment concentrated in denser, transit-served corridors. Likewise, curb-ramp retrofits remain a priority in older, lower-resourced areas with degraded sidewalks predating accessibility standards [14]. More broadly, computer vision applied to street-view imagery supports scalable monitoring for environmental equity and can help target investment across regions [19, 20, 47, 48].

To our knowledge, this study is among the first to assess nine microscale PEFs simultaneously across four U.S. regions using computer vision on more than 20 million street-view images, with classifiers retrained for these regions. Testing walkability as a moderator revealed inequities that main-effects models would miss. The principal interaction findings were broadly

robust across three sensitivity specifications and bootstrap inference (Supplementary Tables S3 and S4), although the curb-cut, buffer, bike-symbol, and zebra-crosswalk interactions did not hold under every specification and should be interpreted with caution.

This study has several limitations. First, the cross-sectional, ecological design cannot support causal inference or generalization to individuals. Second, the street-view imagery and ACS estimates were not perfectly contemporaneous, and image availability can bias streetscape estimates, although many of the measured features change infrequently. Third, our measures capture the presence and quantity of features, not their quality, condition, or connectivity, which equity-focused audits have shown to matter [14]. Fourth, classifier misclassification may vary across features and contexts, although retraining on images stratified by income and walkability was intended to limit such bias; the rule used to aggregate directional images may affect estimated coverage; and the models do not account for spatial autocorrelation among contiguous block groups, which bootstrap resampling does not address. Fifth, the income × walkability interactions explained only a small share of variance ($\Delta R^2 \leq 0.005$), describing the patterning of feature coverage rather than much of its total variation. Finally, the four regions were not selected to be nationally representative, so generalization to other regions and other dimensions of socioeconomic status should be made with caution. Future research could use longitudinal street-view imagery to track change, measure feature quality and condition, apply spatially explicit models, and link feature coverage to walking behavior and health outcomes across larger, more representative sets of regions.

5. Conclusions

Applying computer vision to 5,509 census block groups in four U.S. regions, this study found that income-related differences in microscale pedestrian infrastructure were feature-specific and, for eight of the nine features, conditional on macroscale walkability. Within the most walkable neighborhoods, higher income was associated with greater coverage of basic walking surfaces—sidewalks, curb cuts, and buffers—but with fewer walking safety features and amenities: marked crossings, walk signals, and benches. Macroscale measures can therefore obscure microscale inequities. Pedestrian infrastructure equity should be evaluated feature by feature,

and investment should be matched to pedestrian need, particularly where lower-income residents face elevated injury risk, rather than assumed adequate wherever walkability is high.

Acknowledgements

This work was supported by the National Cancer Institute (https://www.cancer.gov) [R01CA198915-02S1 to MAA; R21CA293976 to MAA] and the National Heart, Lung, and Blood Institute (https://www.nhlbi.nih.gov) [R43HL169137 to James Chapman, Urban Design 4 Health, Inc.] of the National Institutes of Health. The funders had no role in study design, data collection and analysis, decision to publish, or preparation of the manuscript. The content is solely the responsibility of the authors and does not necessarily represent the official views of the National Institutes of Health.

Data availability

The sociodemographic, boundary, and walkability data used in this study are publicly available from the U.S. Census Bureau (American Community Survey, cartographic boundary files, and TIGER/Line shapefiles) and the U.S. Environmental Protection Agency Smart Location Database [32]. The derived block group–level feature coverage measures are available from the corresponding author upon reasonable request.

Declarations

Competing interests: The authors declare that they have no known competing financial interests or personal relationships that could have appeared to influence the work reported in this paper.

Ethics approval: Not applicable. This study used publicly available, area-level data and street-view imagery and did not involve human participants.

Use of AI tools: During the preparation of this work, the authors used a generative AI tool for language editing. The authors reviewed and edited the content as needed and take full responsibility for the article's content.

Author contributions: Zahra Mohammadibalini: Conceptualization, Methodology, Formal analysis, Data curation, Visualization, Writing – original draft, Writing – review and editing. Akshar Patel: Software, Data curation, Writing – review and editing. Christine B. Phillips:

Writing – review and editing. Lawrence D. Frank: Writing – review and editing. Marc A. Adams: Conceptualization, Methodology, Funding acquisition, Project administration, Resources, Supervision, Writing – review and editing.

References

1. Franzini L, Taylor W, Elliott MN, et al. Neighborhood characteristics favorable to outdoor physical activity: disparities by socioeconomic and racial/ethnic composition. Health & place. 2010;16(2):267–274. https://doi.org/10.1016/j.healthplace.2009.10.009
2. Laddu D, Paluch AE, LaMonte MJ. The role of the built environment in promoting movement and physical activity across the lifespan: Implications for public health. Progress in cardiovascular diseases. 2021;64:33–40. https://doi.org/10.1016/j.pcad.2020.12.009
3. Saelens BE, Handy SL. Built environment correlates of walking: a review. Medicine and science in sports and exercise. 2008;40(7 Suppl):S550–S566. https://doi.org/10.1249/MSS.0b013e31817c67a4
4. Smith M, Hosking J, Woodward A, et al. Systematic literature review of built environment effects on physical activity and active transport–an update and new findings on health equity. International journal of behavioral nutrition and physical activity. 2017;14(1):158. https://doi.org/10.1186/s12966-017-0613-9
5. Adams MA, Ryan S, Kerr J, et al. Validation of the Neighborhood Environment Walkability Scale (NEWS) items using geographic information systems. Journal of physical activity and health. 2009;6(s1):S113–S123. https://doi.org/10.1123/jpah.6.s1.s113
6. Conderino SE, Feldman JM, Spoer B, Gourevitch MN, Thorpe LE. Social and economic differences in neighborhood walkability across 500 US cities. American journal of preventive medicine. 2021;61(3):394–401. https://doi.org/10.1016/j.amepre.2021.03.014
7. Frank LD, Appleyard BS, Ulmer JM, Chapman JE, Fox EH. Comparing walkability methods: Creation of street smart walk score and efficacy of a code-based 3D walkability index. Journal of Transport & Health. 2021;21:101005. https://doi.org/10.1016/j.jth.2020.101005
8. Braun LM, Fox EH, Frank LD. Is walkability healthy for all? Using the National Environmental Database to examine equity in the environmental health characteristics of pedestrian-supportive neighborhoods in the US. Social Science & Medicine. 2025;374:118024. https://doi.org/10.1016/j.socscimed.2025.118024
9. Ki D, Chen Z. Walkability inequity in Los Angeles: Uncovering the overlooked role of micro-level features. Transportation research part D: transport and environment. 2023;122:103888. https://doi.org/10.1016/j.trd.2023.103888
10. Cain KL, Gavand KA, Conway TL, et al. Developing and validating an abbreviated version of the Microscale Audit for Pedestrian Streetscapes (MAPS-Abbreviated). Journal of Transport & Health. 2017;5:84–96. https://doi.org/10.1016/j.jth.2017.05.004
11. Cain KL, Millstein RA, Sallis JF, et al. Contribution of streetscape audits to explanation of physical activity in four age groups based on the Microscale Audit of Pedestrian Streetscapes (MAPS). Social science & medicine. 2014;116:82–92. https://doi.org/10.1016/j.socscimed.2014.06.042
12. Sallis JF, Cain KL, Conway TL, et al. Is your neighborhood designed to support physical activity? A brief streetscape audit tool. Preventing chronic disease. 2015;12:E141. https://doi.org/10.5888/pcd12.150098
13. Iroz-Elardo N, Schoner J, Fox EH, Brookes A, Frank LD. Active travel and social justice: Addressing disparities and promoting health equity through a novel approach to Regional Transportation Planning. Social science & medicine. 2020;261:113211. https://doi.org/10.1016/j.socscimed.2020.113211
14. Rajaee M, Echeverri B, Zuchowicz Z, Wiltfang K, Lucarelli JF. Socioeconomic and racial disparities of sidewalk quality in a traditional rust belt city. SSM-population health. 2021;16:100975. https://doi.org/10.1016/j.ssmph.2021.100975

15. Sallis JF, Slymen DJ, Conway TL, et al. Income disparities in perceived neighborhood built and social environment attributes. Health & place. 2011;17(6):1274–1283. https://doi.org/10.1016/j.healthplace.2011.02.006

16. Thornton CM, Conway TL, Cain KL, et al. Disparities in pedestrian streetscape environments by income and race/ethnicity. SSM-population health. 2016;2:206–216. https://doi.org/10.1016/j.ssmph.2016.03.004

17. Kraycheva E, Negm H, Badami MG, El-Geneidy A. Are all streets created equal? Measuring the differences in the built environment among streets with various socioeconomic characteristics in Montréal, Canada. Case Studies on Transport Policy. 2025;19:101349. https://doi.org/10.1016/j.cstp.2024.101349

18. Lubitow A, Rainer J, Bassett S. Exclusion and vulnerability on public transit: experiences of transit dependent riders in Portland, Oregon. Mobilities. 2017;12(6):924–937. https://doi.org/10.1080/17450101.2016.1253816

19. Adams MA, Phillips CB, Patel A, Middel A. Training computers to see the built environment related to physical activity: detection of microscale walkability features using computer vision. International journal of environmental research and public health. 2022;19(8):4548. https://doi.org/10.3390/ijerph19084548

20. Dai S, Li Y, Stein A, Yang S, Jia P. Street view imagery-based built environment auditing tools: a systematic review. International Journal of Geographical Information Science. 2024;38(6):1136–1157. https://doi.org/10.1080/13658816.2024.2336034

21. Koo BW, Guhathakurta S, Botchwey N. How are neighborhood and street-level walkability factors associated with walking behaviors? A big data approach using street view images. Environment and Behavior. 2022;54(1):211–241. https://doi.org/10.1177/00139165211014609

22. Rzotkiewicz A, Pearson AL, Dougherty BV, Shortridge A, Wilson N. Systematic review of the use of Google Street View in health research: Major themes, strengths, weaknesses and possibilities for future research. Health & place. 2018;52:240–246. https://doi.org/10.1016/j.healthplace.2018.07.001

23. Nguyen QC, Huang Y, Kumar A, et al. Using 164 million google street view images to derive built environment predictors of COVID-19 cases. International journal of environmental research and public health. 2020;17(17):6359. https://doi.org/10.3390/ijerph17176359

24. Yang Y, Cho A, Nguyen Q, Nsoesie EO. Association of neighborhood racial and ethnic composition and historical redlining with built environment indicators derived from street view images in the US. JAMA Network Open. 2023;6(1):e2251201. https://doi.org/10.1001/jamanetworkopen.2022.51201

25. Zhou H, He S, Cai Y, Wang M, Su S. Social inequalities in neighborhood visual walkability: Using street view imagery and deep learning technologies to facilitate healthy city planning. Sustainable cities and society. 2019;50:101605. https://doi.org/10.1016/j.scs.2019.101605

26. Favarão Leão AL, Wang Y, Banda BF, et al. Exploring Spatial Inequities and Livability: A Mixed-Methods Study Using Artificial Intelligence and Community Insights. Journal of Urban Health. 2026:1–16. https://doi.org/10.1007/s11524-026-01170-3

27. Lee BA, Farrell CR, Reardon SF, Matthews SA. From census tracts to local environments: An egocentric approach to neighborhood racial change. Spatial Demography. 2018;7(1):1. https://doi.org/10.1007/s40980-018-0044-5

28. U.S. Census Bureau. Geography Program Glossary. Available at: https://www.census.gov/programs-surveys/geography/about/glossary.html. Accessed 4 June 2025.

29. U.S. Census Bureau. TIGER/Line shapefiles: Address range-feature (ADDRFEAT). Available at: https://www.census.gov/geographies/mapping-files/time-series/geo/tiger-line-file.html. Accessed 1 June 2025.

30. U.S. Census Bureau. American Community Survey 5-year estimates, 2019–2023: Detailed tables (block group level). Available at: https://www.census.gov/programs-surveys/acs/news/data-releases/2023/release.html. Accessed 20 June 2025.

31. Thomas J, Zeller L, Reyes A. National walkability index methodology and user guide. Washington, DC: U.S. Environmental Protection Agency; 2021.

32. U.S. Environmental Protection Agency. Smart Location Mapping. Available at: https://www.epa.gov/smartgrowth/smart-location-mapping. Accessed 25 June 2025.

33. U.S. Census Bureau. Cartographic Boundary Files, 2023: Block Groups, 1:500,000. Available at: https://www.census.gov/geographies/mapping-files/time-series/geo/cartographic-boundary.2023.html. Accessed 12 June 2025.

34. Bulmer MG. *Principles of Statistics*. Mineola, NY: Dover Publications; 1979.

35. Aiken LS, West SG. *Multiple Regression: Testing and Interpreting Interactions*. Newbury Park, CA, USA: Sage Publications; 1991.

36. Iacobucci D, Schneider MJ, Popovich DL, Bakamitsos GA. Mean centering helps alleviate "micro" but not "macro" multicollinearity. Behavior Research Methods. 2016;48(4):1308–1317. https://doi.org/10.3758/s13428-015-0624-x

37. Aguinis H, Gottfredson RK, Joo H. Best-practice recommendations for defining, identifying, and handling outliers. Organizational Research Methods. 2013;16(2):270–301. https://doi.org/10.1177/1094428112470848

38. Bollen KA, Jackman RW. Regression diagnostics: An expository treatment of outliers and influential cases. Sociological Methods & Research. 1985;13(4):510–542. https://doi.org/10.1177/0049124185013004004

39. Cook RD. Detection of influential observation in linear regression. Technometrics. 1977;19(1):15–18. https://doi.org/10.1080/00401706.1977.10489493

40. Hesterberg TC. What teachers should know about the bootstrap: Resampling in the undergraduate statistics curriculum. The American Statistician. 2015;69(4):371–386. https://doi.org/10.1080/00031305.2015.1089789

41. Dumbaugh E, Li Y, Saha D, Marshall W. Why do lower-income areas experience worse road safety outcomes? Examining the role of the built environment in Orange County, Florida. Transportation Research Interdisciplinary Perspectives. 2022;16:100696. https://doi.org/10.1016/j.trip.2022.100696

42. Braun LM. Different slopes for different folks: Variations in walkability-walking associations across sociodemographic groups. Transportation Research Part D: Transport and Environment. 2025;147:104914. https://doi.org/10.1016/j.trd.2025.104914

43. Adkins A, Makarewicz C, Scanze M, Ingram M, Luhr G. Contextualizing walkability: do relationships between built environments and walking vary by socioeconomic context? Journal of the American planning association. 2017;83(3):296–314. https://doi.org/10.1080/01944363.2017.1322527

44. Rodrigue L, El-Geneidy A, Manaugh K. Sociodemographic matters: Analyzing interactions of individuals' characteristics with walkability when modelling walking behavior. Journal of transport geography. 2024;114:103788. https://doi.org/10.1016/j.jtrangeo.2023.103788

45. Roll J, McNeil N. Race and income disparities in pedestrian injuries: Factors influencing pedestrian safety inequity. Transportation research part D: transport and environment. 2022;107:103294. https://doi.org/10.1016/j.trd.2022.103294

46. Smart Growth America, National Complete Streets Coalition. *Dangerous by design 2024.* Washington, DC: Smart Growth America; 2024.

47. Huang X, Zeng L, Liang H, Li D, Yang X, Zhang B. Comprehensive walkability assessment of urban pedestrian environments using big data and deep learning techniques. Scientific Reports. 2024;14(1):26993. https://doi.org/10.1038/s41598-024-78041-x

48. Larkin A, Huang T, Chen L, et al. Developing Nationwide Estimates of Built Environment Quality Characteristics Using Street-View Imagery and Computer Vision. Environmental Science & Technology. 2025;59(27):13638–13646. https://doi.org/10.1021/acs.est.5c00966

Table 1 Descriptive characteristics of census block groups by study region

Variable	Phoenix (n = 2,650, 48.1%)	San Diego (n = 1,581, 28.7%)	Baltimore (n = 698, 12.7%)	Seattle (n = 580, 10.5%)	Total (N = 5,509)
Walkability category, n (%)					
Least walkable	239 (9.0)	47 (3.0)	15 (2.1)	0 (0.0)	301 (5.5)
Below-average walkable	811 (30.6)	427 (27.0)	89 (12.8)	15 (2.6)	1,342 (24.4)
Above-average walkable	1,270 (47.9)	734 (46.4)	394 (56.4)	230 (39.7)	2,628 (47.7)
Most walkable	330 (12.5)	373 (23.6)	200 (28.7)	335 (57.8)	1,238 (22.5)
Socioeconomic and demographic predictors, median (Q1–Q3)					
Sex ratio (males per 100 females)	97.95 (83.42–115.51)	99.55 (84.59–118.06)	90.44 (72.97–111.25)	102.28 (86.36–121.61)	98.09 (82.81–116.51)
Population aged 65+ (%)	12.18 (7.05–21.23)	13.92 (8.77–20.61)	15.24 (8.92–21.82)	12.48 (7.32–17.71)	13.18 (7.70–20.73)
Non-White-to-White population ratio	0.44 (0.22–1.02)	0.78 (0.37–1.73)	1.42 (0.38–7.43)	0.53 (0.30–1.00)	0.58 (0.28–1.42)
Hispanic/Latino-to-non-Hispanic/Latino population ratio	0.27 (0.11–0.78)	0.31 (0.14–0.86)	0.04 (0.00–0.11)	0.07 (0.04–0.13)	0.20 (0.07–0.58)
Median household income ($)	88,230 (62,901–119,093)	108,125 (78,232–147,900)	75,769 (53,737–108,583)	129,983 (93,337–168,750)	95,227 (67,126–132,323)
National Walkability Index (1–20), mean (SD)	11.13 (3.59)	12.38 (3.53)	13.41 (3.13)	15.57 (2.38)	12.24 (3.68)
Microscale pedestrian environment features (% coverage), median (Q1–Q3)					
Measured over all sampling points					
Sidewalk	93.65 (74.28–99.74)	83.52 (67.21–97.58)	90.45 (75.32–98.04)	81.26 (58.81–95.59)	89.67 (70.41–99.05)
Buffer	15.29 (7.26–29.58)	27.77 (11.70–56.33)	64.69 (46.69–77.78)	64.41 (35.67–87.55)	25.73 (10.61–56.73)
Bike symbol	0.64 (0.08–1.98)	1.11 (0.37–2.88)	0.23 (0.00–1.15)	2.75 (0.36–5.90)	0.79 (0.13–2.53)
Streetlight	78.60 (66.49–88.95)	58.23 (47.17–71.22)	72.31 (58.02–82.21)	62.85 (52.79–71.58)	70.45 (55.55–83.00)
Bench	1.28 (0.67–2.22)	1.51 (0.85–2.84)	1.26 (0.68–2.07)	1.65 (0.92–3.33)	1.37 (0.73–2.43)
Measured over intersection sampling points					
Curb cut	57.07 (42.84–66.51)	56.68 (44.38–65.94)	51.23 (38.89–60.21)	41.34 (29.71–53.25)	54.72 (40.53–65.17)
Line crosswalk	4.91 (2.46–9.56)	7.41 (3.59–13.85)	5.08 (2.13–10.45)	0.00 (0.00–0.89)	4.90 (1.85–10.30)
Zebra crosswalk	0.00 (0.00–0.00)	2.09 (0.00–7.26)	6.59 (1.73–15.35)	12.33 (6.96–21.49)	0.27 (0.00–5.68)
Walk signal	3.14 (1.48–6.36)	6.87 (2.81–13.72)	5.91 (2.22–12.36)	6.00 (2.22–12.11)	4.40 (1.84–10.00)

Note. Q1–Q3 = first–third quartiles; SD = standard deviation. Column headings give the number and percentage of the total analytic sample contributed by each region. Medians and quartiles are reported for right-skewed continuous variables and the mean (SD) for the approximately symmetric National Walkability Index. Microscale pedestrian environment features are expressed as percentage coverage of sampled points. For curb cuts, line crosswalks, zebra crosswalks, and walk signals, coverage is calculated over intersection sampling points only (Section 2.2). N = 5,509 census block groups across the four U.S. study regions.

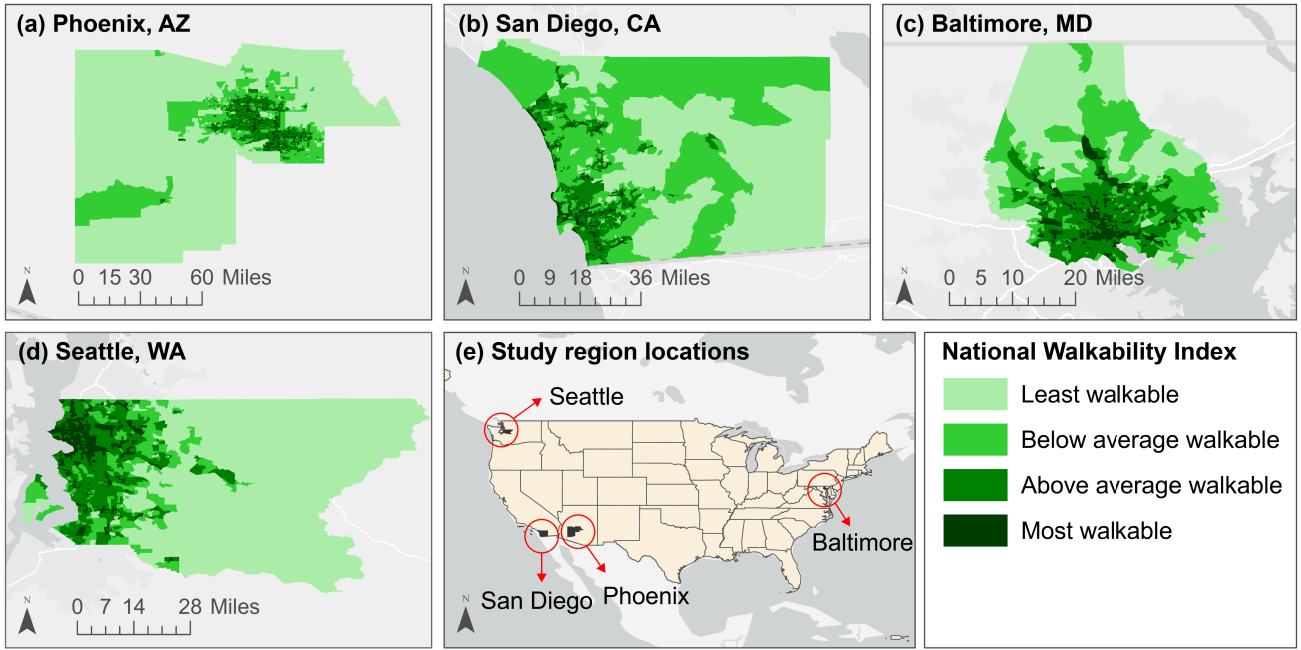
Table 2 Multivariable linear regression interaction models predicting microscale pedestrian environment features (N = 5,509)

Predictor	Sidewalk (%)	Buffer (%)	Bike symbol (%)	Streetlight (%)	Bench (%)	Curb cut (%)	Line crosswalk (%)	Zebra crosswalk (%)	Walk signal (%)
Sex ratio (males per 100 females)	−0.005*** (−0.008, −0.003)	−0.001 (−0.004, 0.002)	0.000 (0.000, 0.000)	−0.005*** (−0.007, −0.002)	0.000 (0.000, 0.000)	−0.003** (−0.005, −0.001)	0.000 (−0.001, 0.001)	0.001 (0.000, 0.002)	0.001 (0.000, 0.002)
Population aged 65+ (%)	−0.058** (−0.098, −0.018)	−0.166*** (−0.210, −0.122)	−0.006* (−0.012, 0.000)	−0.178*** (−0.211, −0.145)	0.000 (−0.003, 0.004)	−0.112*** (−0.144, −0.079)	0.029** (0.011, 0.047)	−0.005 (−0.020, 0.011)	0.015 (−0.005, 0.035)
Non-White-to-White population ratio	0.026* (0.005, 0.046)	0.031** (0.008, 0.054)	−0.002 (−0.005, 0.001)	0.008 (−0.009, 0.025)	−0.001 (−0.003, 0.001)	0.024** (0.008, 0.041)	−0.008 (−0.018, 0.001)	0.007 (−0.001, 0.015)	−0.005 (−0.016, 0.005)
Hispanic/Latino-to-non-Hispanic/Latino population ratio	−0.079 (−0.270, 0.111)	−0.436*** (−0.646, −0.226)	−0.074*** (−0.102, −0.046)	−0.109 (−0.267, 0.048)	−0.014 (−0.032, 0.004)	−0.153 (−0.307, 0.000)	−0.067 (−0.153, 0.020)	−0.068 (−0.143, 0.007)	−0.163*** (−0.259, −0.067)
Region (Ref: Phoenix)									
San Diego	−6.490*** (−7.904, −5.077)	11.074*** (9.516, 12.632)	0.851*** (0.642, 1.061)	−16.279*** (−17.448, −15.111)	0.364*** (0.229, 0.499)	−0.869 (−2.006, 0.268)	2.344*** (1.703, 2.985)	4.474*** (3.918, 5.029)	4.652*** (3.939, 5.365)
Seattle	−16.136*** (−18.383, −13.888)	31.440*** (28.964, 33.916)	2.140*** (1.807, 2.472)	−17.000*** (−18.857, −15.142)	0.049 (−0.166, 0.263)	−16.721*** (−18.528, −14.914)	−8.457*** (−9.475, −7.438)	15.652*** (14.769, 16.535)	3.513*** (2.380, 4.647)
Baltimore	−4.320*** (−6.213, −2.427)	36.488*** (34.402, 38.574)	−0.358* (−0.638, −0.078)	−8.916*** (−10.481, −7.352)	−0.537*** (−0.718, −0.357)	−7.483*** (−9.005, −5.961)	−2.099*** (−2.957, −1.241)	8.890*** (8.146, 9.634)	1.416** (0.462, 2.371)
Median household income (per $10,000)	−0.019 (−0.148, 0.110)	0.378*** (0.236, 0.521)	0.015 (−0.005, 0.034)	−0.754*** (−0.861, −0.647)	−0.041*** (−0.054, −0.029)	−0.088 (−0.192, 0.015)	−0.213*** (−0.272, −0.155)	−0.123*** (−0.173, −0.072)	−0.317*** (−0.382, −0.252)
National Walkability Index (1–20)	1.759*** (1.577, 1.940)	0.761*** (0.561, 0.962)	0.123*** (0.096, 0.150)	1.265*** (1.114, 1.415)	0.219*** (0.201, 0.236)	1.076*** (0.930, 1.222)	0.615*** (0.532, 0.697)	0.561*** (0.490, 0.632)	0.777*** (0.685, 0.869)
Median household income × National Walkability Index	0.081*** (0.050, 0.113)	0.044* (0.009, 0.079)	−0.006* (−0.010, −0.001)	0.022 (−0.004, 0.049)	−0.006*** (−0.009, −0.003)	0.033* (0.007, 0.058)	−0.033*** (−0.047, −0.019)	−0.016** (−0.029, −0.004)	−0.045*** (−0.061, −0.029)
R^2	0.100	0.305	0.090	0.246	0.151	0.101	0.124	0.337	0.125
Adjusted R^2	0.098	0.303	0.088	0.245	0.150	0.100	0.123	0.336	0.123
ΔR^2 (interaction term)	0.004***	0.001*	0.001*	0.000	0.002***	0.001*	0.003***	0.001**	0.005***

Note. Cell entries are unstandardized regression coefficients (B) with 95% confidence intervals (in parentheses) from the income × walkability interaction model for each outcome. Outcomes are census block-group percentage coverage of each microscale pedestrian environment feature. Median household income was rescaled in $10,000 units, and both income and the National Walkability Index (originally scored 1–20) were mean-centered before computing the interaction term; coefficients therefore reflect the change in percentage-point coverage per $10,000 increase in income and per 1-point increase in the Walkability Index, and lower-order coefficients represent associations at the sample mean of the other variable. Phoenix is the reference region. ΔR^2 is the increment in R^2 from adding the interaction term. All variance inflation factors < 1.5; N = 5,509 block groups for all models. Full main-effects models (Model 1) are reported in Supplementary Table S2. * $p < .05$, ** $p < .01$, *** $p < .001$.

Fig. 1 Study regions and neighborhood walkability. Panels (a) Phoenix (Maricopa County, AZ); (b) San Diego (San Diego County, CA); (c) Baltimore (Baltimore City and Baltimore County, MD); and (d) Seattle (King County, WA) show census block groups by National Walkability Index category: least walkable (1.0–5.75), below-average (5.76–10.5), above-average (10.51–15.25), and most walkable (15.26–20.0). Panel (e) shows the study regions within the contiguous United States. Categories are shown for visualization only; the continuous index was used in all analyses. Data: U.S. Environmental Protection Agency Smart Location Database; U.S. Census Bureau cartographic boundary files. Basemap: Esri, TomTom, Garmin, FAO, NOAA, USGS, © OpenStreetMap contributors, and the GIS User Community. Map lines delineate study areas and do not necessarily depict accepted national boundaries

Fig. 2 Model-predicted coverage of nine microscale pedestrian environment features by median household income and walkability category. Predicted values are from the income × walkability interaction models (Table 2), with covariates held at their sample means. Lines denote walkability categories, distinguished by shading (light to dark) and line style: least (dotted), below-average (dash-dot), above-average (dashed), and most walkable (solid); thinner flanking lines show 95% confidence bands. Lines span the 5th–95th income percentiles within each category. Y-axis scales differ across panels


(a) Phoenix, AZ
N
0 15 30 60 Miles
(b) San Diego, CA
N
0 9 18 36 Miles
(c) Baltimore, MD
N
0 5 10 20 Miles
(d) Seattle, WA
N
0 7 14 28 Miles
(e) Study region locations
Seattle
Baltimore
San Diego
Phoenix
N
National Walkability Index
Least walkable
Below average walkable
Above average walkable
Most walkable

Supplementary Files

This is a list of supplementary files associated with this preprint. Click to download.

- SupplementaryInformation.docx